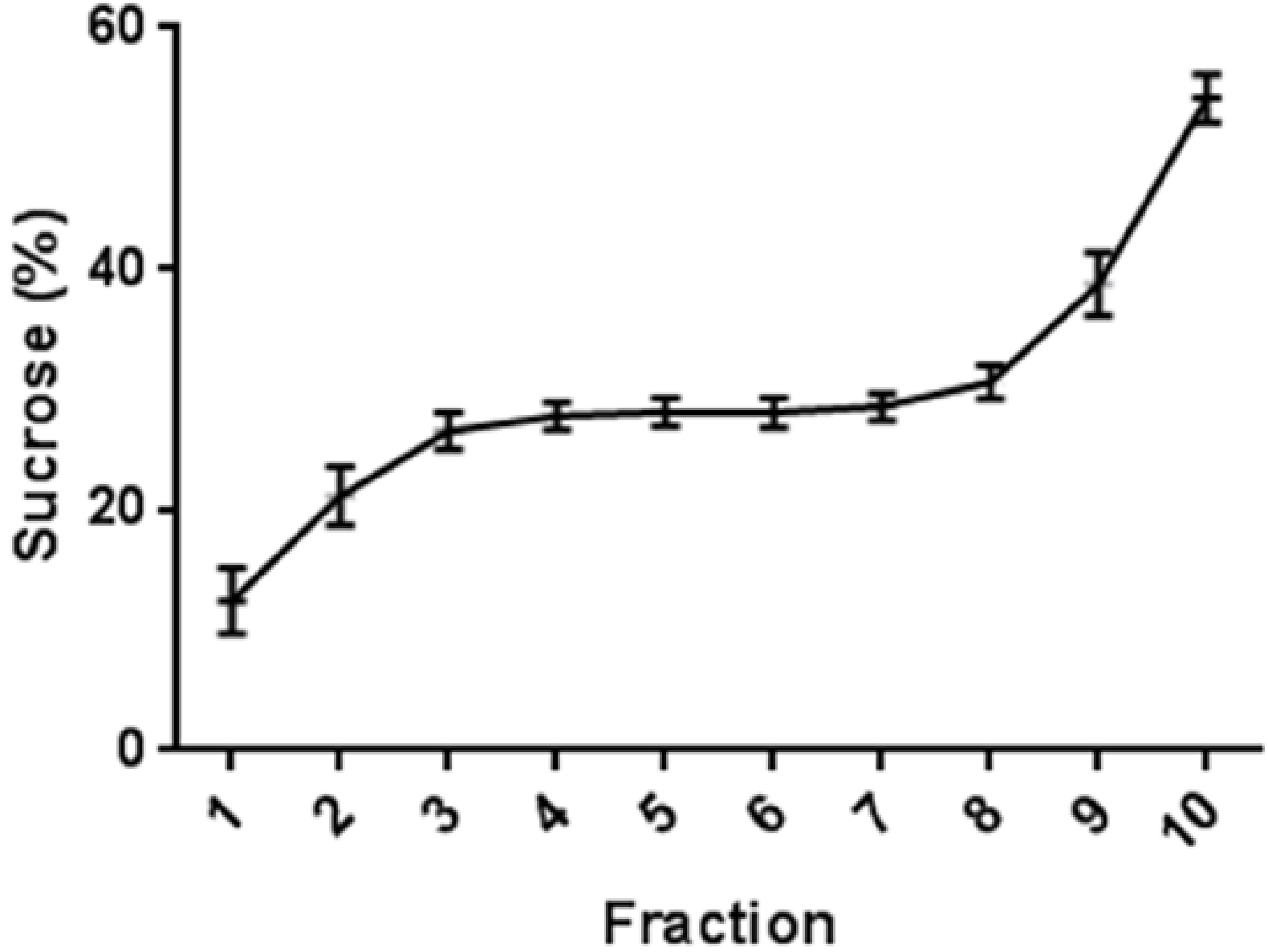

Supplementary 1

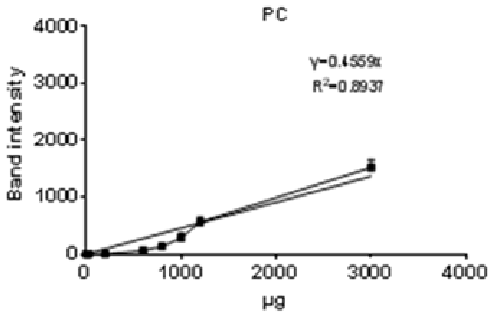

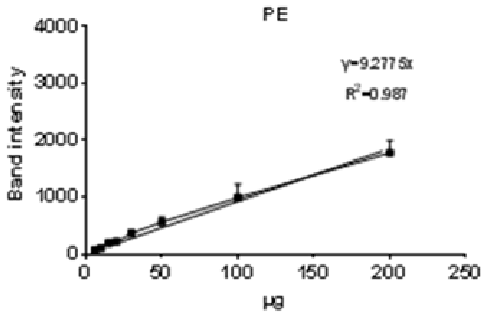

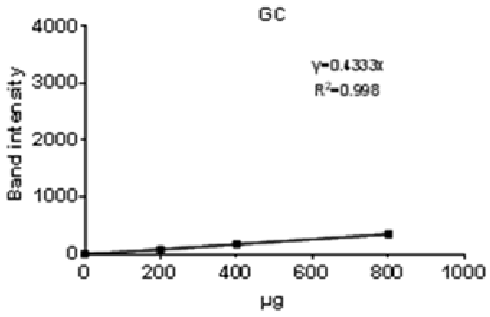

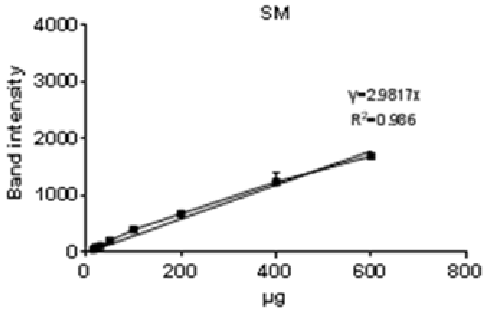

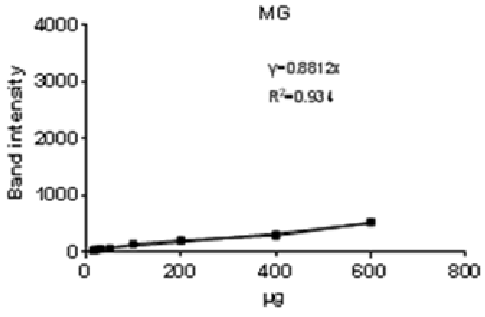

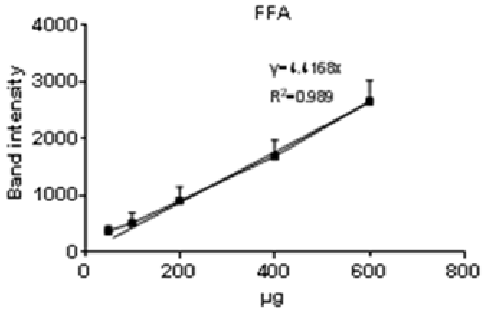

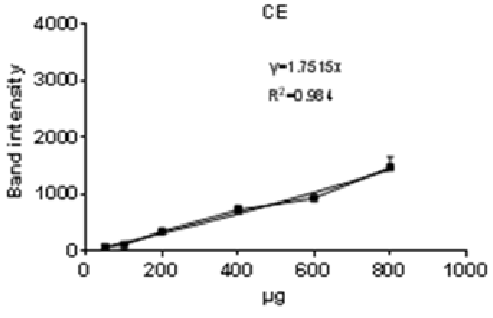

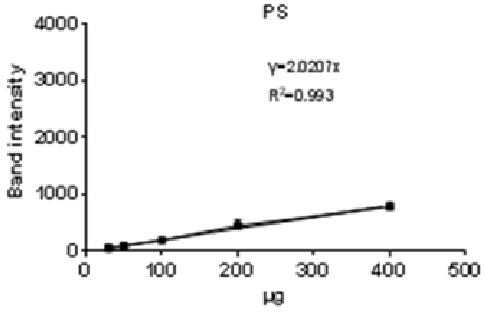

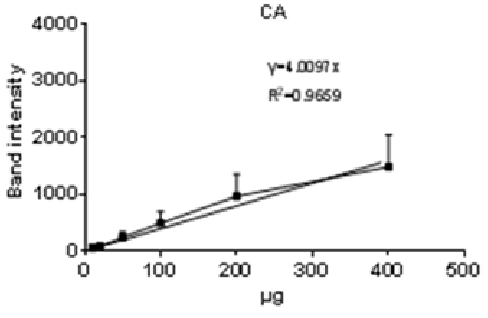

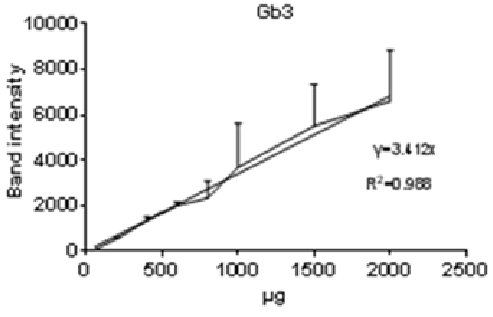

Supplementary 2

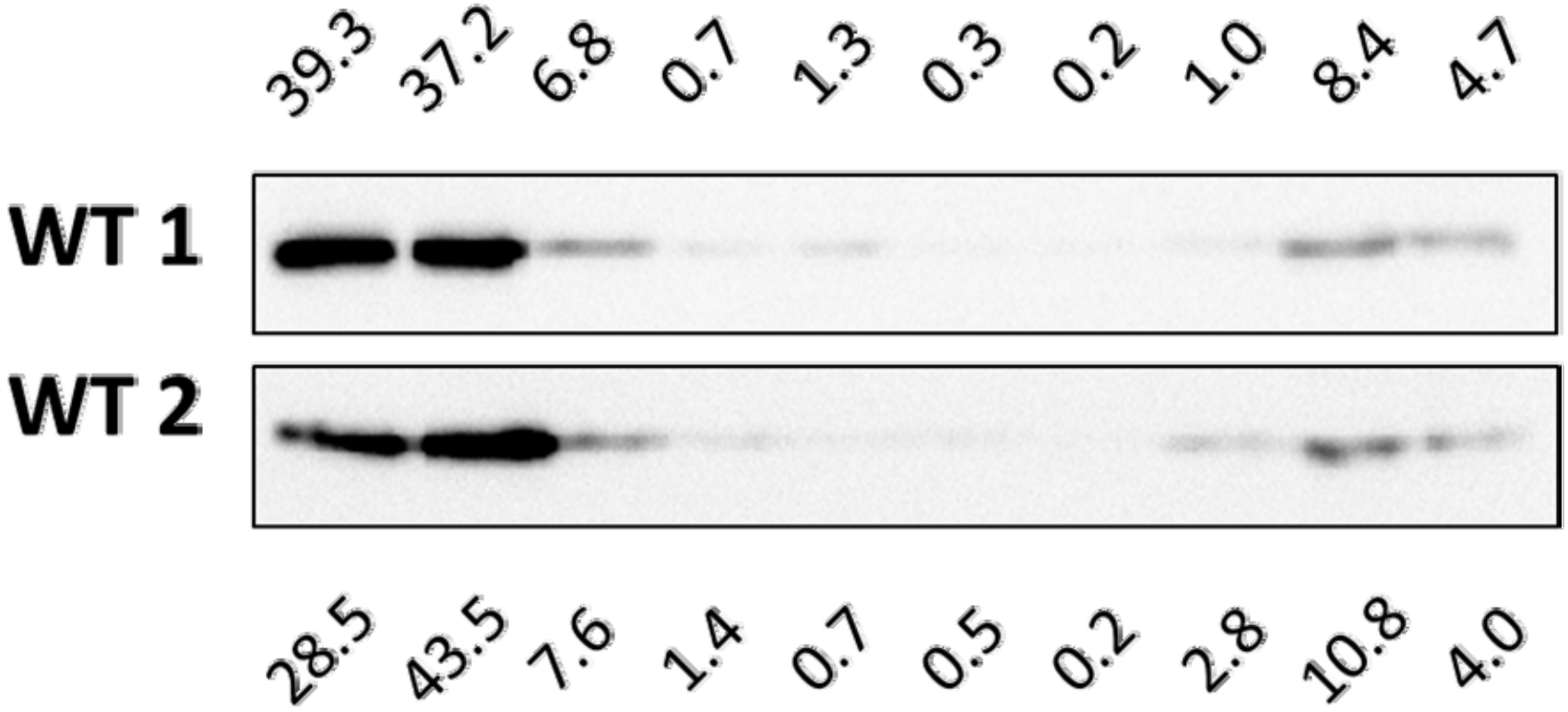

Supplementary 3

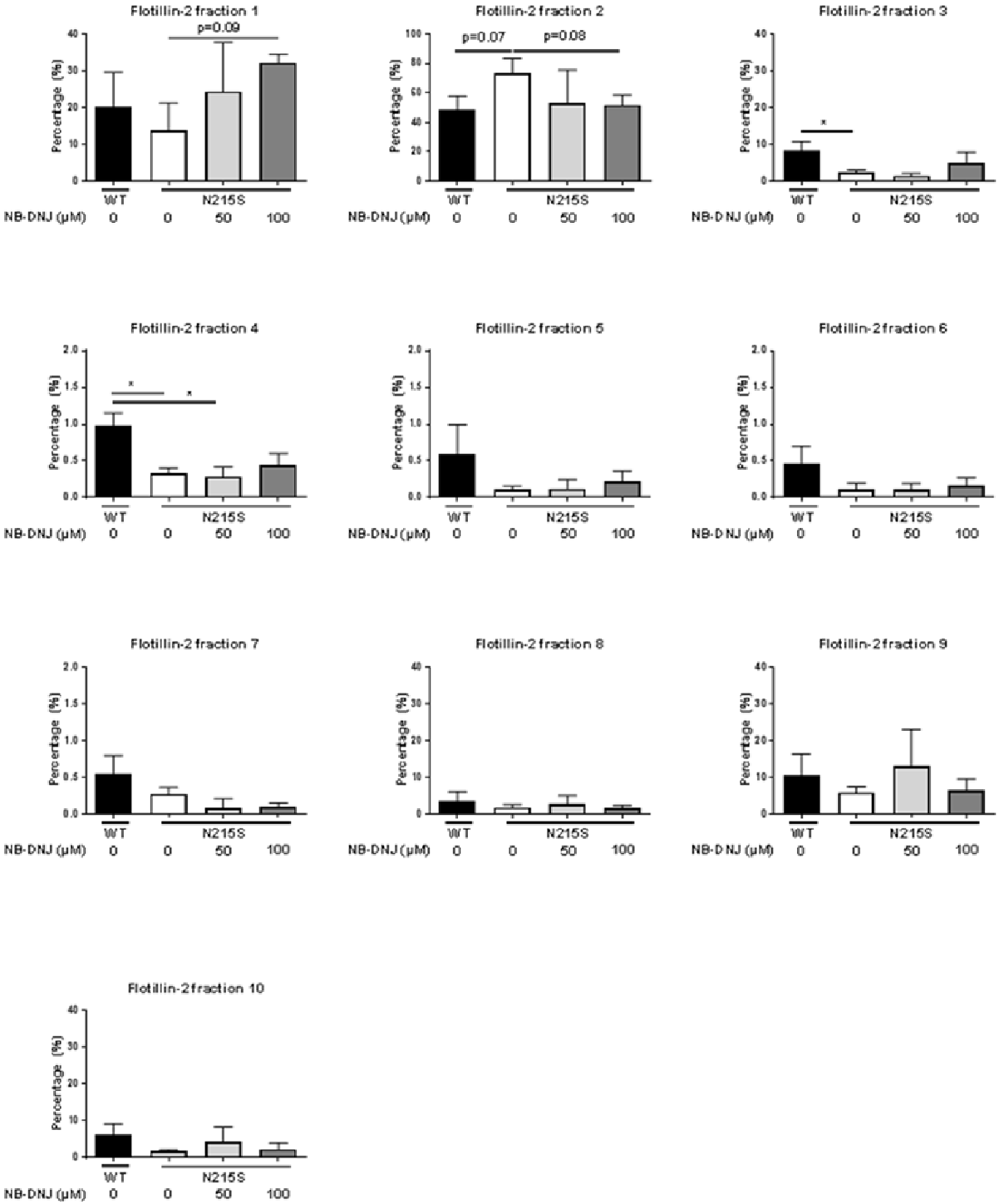

Supplementary 4

Fraction / NB-DNJ	WT	N215S		
		0	50	100
1	20.1 ±16.5	13.8±12.9	24.4±13.4	32.2±4.1
2	48.5±16.3	73.5±17.6	53.5±22.2	51.6±12.0
3	8.5±4.1	2.4±0.9	1.4±0.6	4.9±5.4
4	0.9±0.3	0.3±0.1	0.3±0.1	0.6±0.6
5	0.6±0.7	0.1.0.1	0.1±0.1	0.2±0.2
6	0.5±0.4	0.1±0.1	0.1±0.1	0.2±0.2
7	0.5±0.4	0.3±0.2	0.1±0.1	0.1±0.1
8	3.5±4.4	1.8±1.2	2.7±2.3	1.6±1.2
9	10.6±9.8	5.9±2.8	13.1±9.8	6.3±5.5
10	6.2±5.1	1.8±0.5	4.3±4.1	2.3±2.8

Supplementary 5

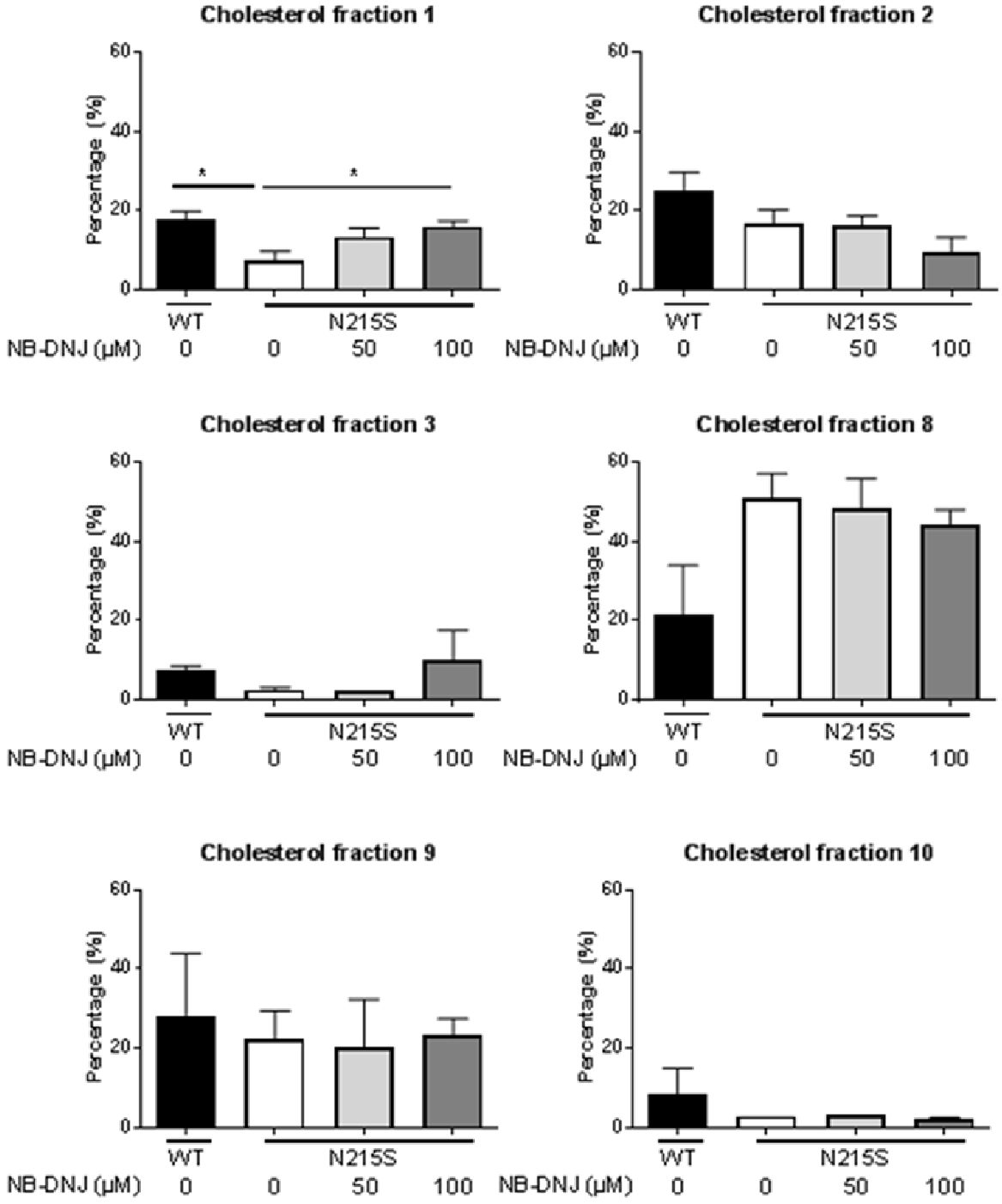

Supplementary 6

Fraction / NB-DNJ	WT	N215S		
		0	50	100
1	18.0 ±2.8	7.6±3.9	13.5±3.7	16.0±2.6
2	25.3±7.5	16.9±5.8	16.2±4.3	9.6±6.3
3	7.3±2.2	2.6±0.8	2.4	10.0±10.7
8	21.5±21.6	50.8±11.0	48.4±12.9	44.1±6.9
9	28.3±15.6	22.1±12.7	20.1±12.2	23.2±4.3
10	8.3±6.7	2.9	3.1	2.1±0.4

Supplementary 7

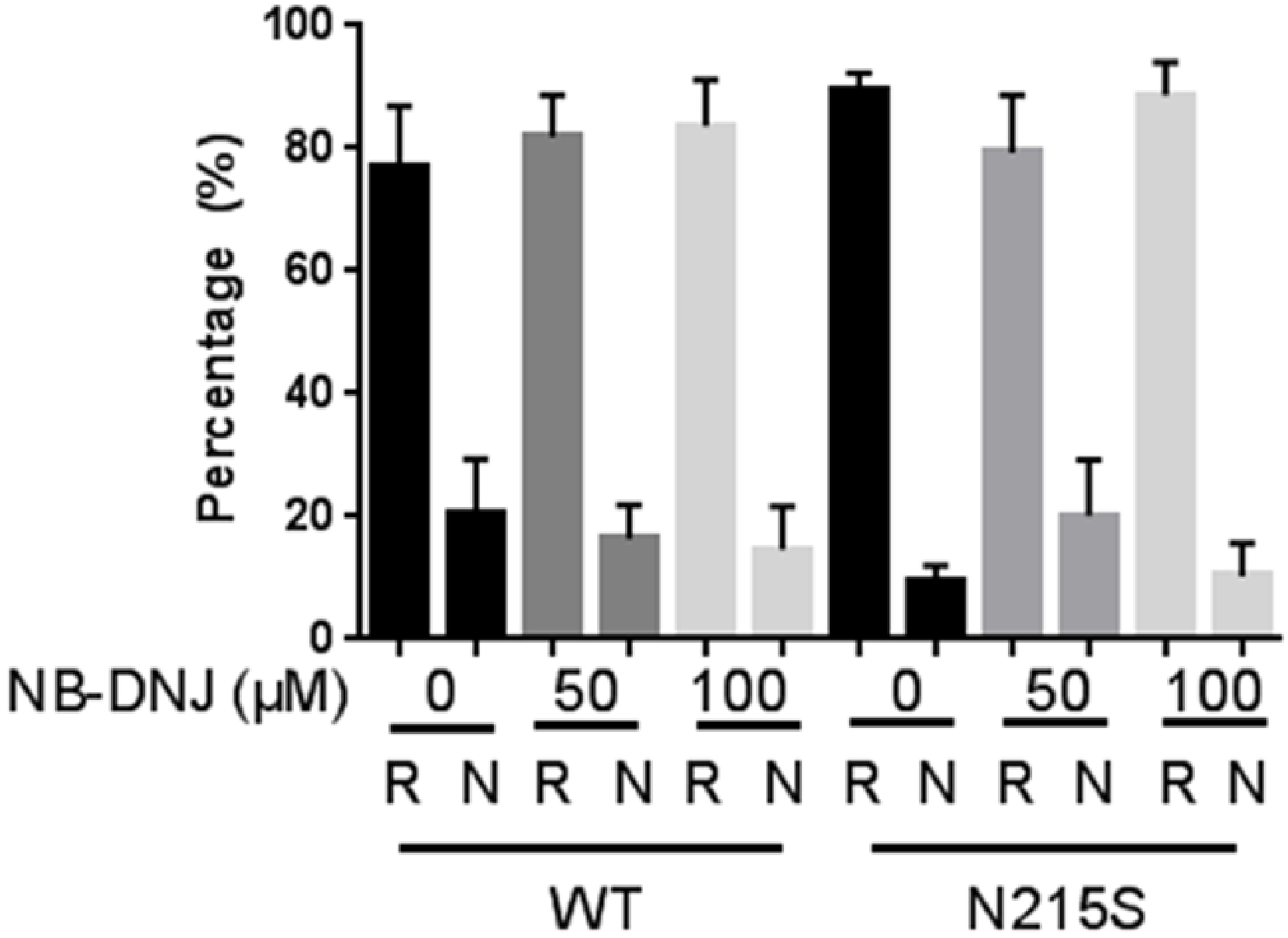

Supplementary 8

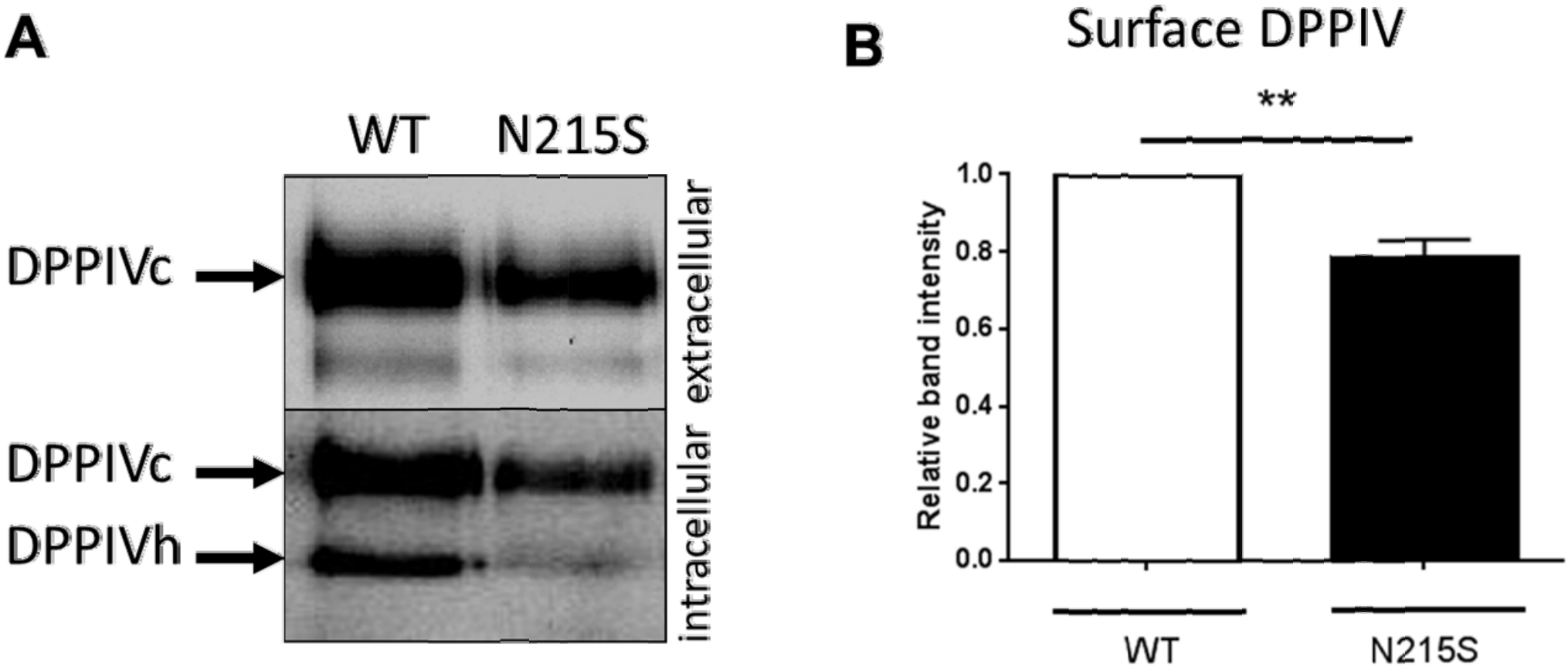

Supplementary 9

Supplementary 1 Distribution of sucrose in the sucrose density gradient. The amount of sucrose in each fraction post centrifugation was analysed. Fraction 1 contained 12.45%, fraction 2 24.6% and fraction 3 26.51% of sucrose, with a standard deviation of 2.7, 2.4 and 1.5 respectively.

Supplementary 2 Standard curves used to quantify lipid concentrations by HPTLC and TLC. Standard curves were produced for 10 different lipids by loading increasing concentrations onto HPTLC plates and for Gb3 TLC plates: Phosphatidylcholine (PC), phosphoethanolamine (PE), galactocerebroside (GC), sphingomyelin (SM), monoacylglycerol (MG), free fatty acids (FFA), cholesterol ester (CE), phosphatidylserine (PS), cardiolipin (CA), Globotriaosylceramide (Gb3). The lowest detection limits and linear ranges were also determined for each lipid. A standard curve used to quantify the lipid concentration of each sample was generated by using at least 5 different values within the linear range. Band intensities acquired for each lipid were only used when they above the minimum detection limit and within the linear range of the corresponding lipid standard.

Supplementary 3 Flotillin-2 distribution from two different wild type fibroblasts. Flotillin-2 distribution (in percentage) from two different wild type fibroblasts showing a higher concentration of the lipid raft-associated protein in fractions 1 and 2. Flotillin 2 distribution for the shown immunoblots are for WT 1; 39.3%, 37.2% and 6.8%, and for WT 2; 28.5%, 43.5% and 7.6% for sucrose fractions 1, 2 and 3 respectively. WT 2, which is closer to the FD fibroblasts, was used in all experiments presented throughout this study as WT.

Supplementary 4 Effect of NB-DNJ on the flotillin-2 distribution in sucrose density gradient fractions isolated from fibroblasts derived from Fabry patients

Fibroblasts derived from a Fabry patient (N215S) or age-matched healthy individuals (WT) were treated with NB-DNJ for three days and were subsequently lysed with 1% (w/v) Triton X-100 and run on density-based sucrose gradients. Ten fractions were collected and

analysed for distribution of flotillin-2 by immunoblotting. The results are displayed as a percentage of the total flotillin-2 detected throughout all 10 fractions. (*p<0.05, ±SD, n=3).

Supplementary 5 Table showing the flotillin-2 distribution in sucrose density gradient fractions isolated from fibroblasts derived from Fabry patients post NB-DNJ treatment

Fibroblasts derived from a Fabry patient (N215S) or age-matched healthy individuals (WT) were treated with NB-DNJ for three days and were subsequently lysed with 1% (w/v) Triton X-100 and run on density-based sucrose gradients. Ten fractions were collected and analysed for distribution of flotillin-2 by immunoblotting. The results are displayed as a percentage of the total flotillin-2 detected throughout all 10 fractions. (*p<0.05, SEM, n=3).

Supplementary 6 Cholesterol distribution in sucrose density gradient fractions

Fibroblasts derived from a Fabry patient (N215S) or age-matched healthy individuals (WT) were treated with NB-DNJ for three days and were subsequently lysed with 1% (w/v) Triton X-100 and run on density-based sucrose gradients. Ten fractions were collected and the cholesterol content was analysed via HPLC. The results are expressed as a percentage of the total cholesterol quantified from the 6 samples analysed, fractions 1, 2, 3 and 8, 9 and 10, which contained cholesterol at concentrations above the minimum detection limit. (*p<0.05, SEM, n=3).

Supplementary 7 Table showing the cholesterol distribution in sucrose density gradient fractions

Fibroblasts derived from a Fabry patient (N215S) or age-matched healthy individuals (WT) were treated with NB-DNJ for three days and were subsequently lysed with 1% (w/v) Triton X-100 and run on density-based sucrose gradients. Ten fractions were collected and the cholesterol content was analysed via HPLC. The results are expressed as a percentage of the total cholesterol quantified from the 6 samples analysed, fractions 1, 2, 3 and 8, 9 and

10, which contained cholesterol at concentrations above the minimum detection limit. (*p<0.05, ±SD, n=3).

Supplementary 8 Fibroblasts derived from a Fabry patient (N215S) or age-matched healthy individuals (WT) were lysed with 1% (w/v) Triton X-100 and run on density-based sucrose gradient. Nine fractions were collected and analysed for distribution of the lipid raft-associated flotillin-2 by immunoblotting. Flotillin-2 distribution was calculated by grouping the lipid raft fractions 1-3 and non-raft fraction 8-10 and shown as a percentage. No significant difference was found in the raft and non-raft flotillin-2 distributions between wild type and Fabry fibroblasts.

Supplementary 9 DPPIV trafficking to the cell surface is impaired in Fabry fibroblasts. Fibroblasts were solubilised in standard lysis buffer. Intra- and extracellular distribution analysis of the lipid raft associated DPPIV protein was performed using biotinylation and Western blotting of the obtained isolate. The results show that the cell surface consists almost entirely of the complex glycosylated form of DPPIV (DPPIVc) in both the wild type and Fabry fibroblasts (A). The intracellularly located DPPIV was present in both complex (upper band) and high mannose (lower band) forms. Lower band intensities of both the DPPIVc and DPPIVh forms of the protein were present in Fabry fibroblasts relative to the wild type fibroblasts. Fabry fibroblasts have lower concentrations of DPPIV on the cell surface compared to wild type cells (B).